Journal Pre-proof

The Ocular Surface
A JOURNAL OF REVIEW, LIVING LABORATORY SCIENCE, CLINICAL SCIENCE, AND CLINICAL PRACTICE

Prior inhibition of AKT phosphorylation by BX795 can define a safer strategy to prevent herpes simplex virus-1 infection of the eye

Tejabhiram Yadavalli, Rahul Suryawanshi, Marwan Ali, Aqsa Iqbal, Raghuram Koganti, Joshua Ames, Vinay Kumar Aakalu, Deepak Shukla

PII: S1542-0124(19)30421-5

DOI: https://doi.org/10.1016/j.jtos.2019.11.011

Reference: JTOS 458

To appear in: *Ocular Surface*

Received Date: 29 October 2019

Revised Date: 15 November 2019

Accepted Date: 22 November 2019

Please cite this article as: Yadavalli T, Suryawanshi R, Ali M, Iqbal A, Koganti R, Ames J, Aakalu VK, Shukla D, Prior inhibition of AKT phosphorylation by BX795 can define a safer strategy to prevent herpes simplex virus-1 infection of the eye, *Ocular Surface* (2019), doi: https://doi.org/10.1016/j.jtos.2019.11.011.

Prior inhibition of AKT phosphorylation by BX795 can define a safer strategy to prevent herpes simplex virus-1 infection of the eye

Tejabhiram Yadavalli[1], Rahul Suryawanshi[1], Marwan Ali[1], Aqsa Iqbal[1], Raghuram Koganti[1,2], Joshua Ames[1,3], Vinay Kumar Aakalu[1], Deepak Shukla[1,3]

[1] *Department of Ophthalmology and Visual Sciences, University of Illinois at Chicago, Chicago, IL 60612, USA*

[2] *College of Liberal Arts and Sciences, University of Illinois at Chicago, Chicago, IL 60612, USA*

[3] *Department of Microbiology and Immunology, University of Illinois at Chicago, Chicago, IL 60612, USA*

Short Title: Prophylactic treatment with BX795 is well-tolerated and inhibits HSV-1

Abstract

Purpose: To evaluate the prophylactic antiviral efficacy, corneal tolerance and toxicity of topically dosed BX795, a non-nucleoside small-molecule inhibitor of herpes simplex virus type-1 (HSV-1).

Methods: Prophylactic treatment with BX795 was performed both *in-vitro* on human corneal epithelial cells and *in-vivo* on mice prior to HSV-1 challenge. Viral burden was evaluated using a standard plaque assay. In a separate experiment, mice were treated topically 3-times daily for 4-weeks with BX795 to evaluate corneal tolerance and toxicity. Phenol-red thread measurements, fluorescein staining and optical coherence tomography (OCT) were used to evaluate tear production, dryness and corneal structural changes. Corneal sensitivity and intraocular pressure were measured using esthesiometery and tonometery respectively.

Results: Both *in-vitro* and *in-vivo* results showed a robust suppression of HSV-1 infection when treated prophylactically with BX795. The fluorescein stain and phenol-red results for the BX795-treated eyes did not show signs of corneal surface dryness when compared to trifluridine (TFT), an FDA-approved topical antiviral. The OCT measurements showed no signs of structural changes to the cornea suggesting that BX795 treatment was well tolerated without any apparent signs of toxicity or inflammation. The corneal sensitivity of BX795-treated eyes was not significantly different from TFT-treated eyes. No significant increase in the intraocular pressure of BX795-treated mice was observed.

Conclusions: Prophylactic treatment with BX795 protects corneal cells from HSV-1 infection. The antiviral is well-tolerated on murine corneas without any detectable toxicity.

Keywords:

BX795; prophylaxis; corneal toxicity; herpes simplex virus; topical

Highlights:

1. Prophylactic treatment with BX795 protects murine corneas from HSV-1 infection
2. The efficacy of the drug is through translational inhibition of viral proteins.
3. Pre-treatment with BX795 down-regulated AKT phosphorylation even during HSV-1 infection.
4. A four-week topical treatment regimen on the ocular surface with BX795 was well-tolerated
5. No significant loss in corneal sensitivity, surface wetness and structural integrity was observed during this period.

Introduction

Herpes simplex virus type-1 (HSV-1) is the main cause of infectious blindness among adults in the USA(1-6). Millions of patients around the world suffer from recurring HSV-1 infections, which can cause irreversible corneal scarring and potential need for corneal transplantation(7-11). HSV-1 has a seroprevalence of 60-90% with almost 100% of people infected by the age of 70(12-15).

A majority of currently approved and commonly used drugs such as acyclovir are nucleoside analogs that target replication of HSV-1 DNA (3, 16-20). However, viral resistance and renal toxicity are relatively common after prolonged usage of acyclovir especially by immunocompromised patients, which highlights the need for novel treatments that can be safely prescribed for therapeutic as well as prophylactic indications in the eye (21-26). While various strategies such as peptides(27, 28), nanoparticles(29, 30) and novel acyclovir delivery systems(31) have been proposed previously, more feasible options with regards to scalability and cost-effectiveness are desired.

Last year we made the serendipitous discovery that BX795 a small molecule TBK-1 inhibitor, shows strong therapeutic efficacy against HSV-1 in an ocular model of infection(32, 33). This promising small molecule inhibitor of HSV-1 blocked viral protein synthesis and showed strong therapeutic efficacy against an acyclovir resistant strain. In several different models, BX795 was very effective as a topical antiviral for ocular infection. While we were able to demonstrate strong therapeutic efficacy, a significant question whether BX795 can also be a novel topical prophylaxis was not addressed.

Here we demonstrate the strong promise of BX795 as a topical prophylactic antiviral for corneal infection. We provide evidence that the mechanism of prophylactic action by BX795 is through the inhibition of PI3K/AKT/mTOR pathway which then blocks hyper-phosphorylation of 4EBP1, crippling the virus from using host cell's protein translational machinery to its own advantage(32). In support of a

promising topical prophylaxis BX795 is well tolerated on the cornea without any detectable toxicity at the effective concentration.

Methods

Cells, viruses, media, and drugs

Human Corneal Epithelial cells (HCEs; RCB1834 HCE-T) and Vero cells were used under previously described growth media and conditions[33].

Two strains of HSV-1 were used in the course of this study: HSV-1 McKrae (34, 35) and HSV-1 17 GFP (36, 37). All viruses were grown and titrated on Vero cells before they were aliquoted and stored at -80 °C for long term storage.

BX795 and trifluridine (TFT) were purchased from Selleckchem, Houston, TX, USA. Stock drug solutions were prepared in DMSO at 10 mM (BX795) and 50 mM (TFT), aliquoted, and stored at -80 °C. A fresh aliquot of drug was opened each time an experiment was planned.

MTT Cytotoxicity Assay

The *in vitro* cytotoxicity of BX795 and TFT was evaluated using a standard MTT assay on HCE cells using a previously published protocol [33]. The intensity of the color developed was analyzed by a Tecan GENios Pro microplate reader at 562 nm. Experiments were conducted using 3 biological replicates.

Propidium iodide staining Assay

Cell death marker, propidium iodide was added to HCEs either treated with BX795/TFT/mock DMSO at a concentration of 2 µg/mL. Cell nuclei were also stained with live cell Hoescht stain (DAPI). The cells were placed in a specially designed live-cell imaging system (Zeiss Spinning Disk) with an incubation chamber

for a period of 72 hours. Images taken every 3 hours were used to calculate number of total and dead cells based on number of cells stained blue or red respectively.

Western Blotting

Immunoblotting was performed using protocols mentioned previously(31). The blots were developed using the ECL Femto/Pico Substrate (ThermoFisher Scientific) and imaged with the Quant 4000 (GE Healthcare). Antibodies and their concentrations are as follows. anti-rabbit GAPDH (Proteintech, 1:1000), anti-rabbit 4EBP1 (Cell Signaling Technologies, 1:1000), anti-rabbit phospho-4EBP1$^{Thr37/46}$ (Cell Signaling Technologies, 1:500), anti-rabbit AKT (Cell Signaling Technologies, 1:1000), anti-rabbit phospho-AKT^{Ser473}(Cell Signaling Technologies, 1:500), anti-mouse P70S6K (SantaCruz Biotechnologies, 1:500), anti-mouse phospho-P70S6K (SantaCruz Biotechnologies, 1:500), anti-mouse HSV-1 gD and ICP0 (Abcam, 1:1000). Horse radish peroxidase tagged secondary anti-rabbit and anti-mouse IgG (Jackson ImmunoResearch, 1:10,000).

Murine mode of ocular HSV-1 infection

All animal care and surgical procedures were performed in accordance with the institutional IACUC protocols approved by the animal care committee at the University of Illinois at Chicago and we confirm adherence to the ARVO Statement for the Use of Animals in Ophthalmic and Vision Research. 6-8 week old male C57BL6 mice were used. Prior to infection, mice were given drops 3 times (8 hours apart) with either PBS, BX795 (10 µM), or TFT (50 µM) before they were anesthetized using ketamine (100 mg/kg) and xylazine (5 mg/kg). Epithelial debridement of the treated eye was carried out with a 30-g sterile needle in a 3 × 3 grid pattern prior to the addition of $5x10^5$ PFU McKrae virus in a total volume of 5 µL/eye (38, 39). Mice were monitored every 24 h, and ocular swabs (for plaque assay) were collected every 48 h for a period of 7 days. On the 7th day post infection, mice were euthanized and their trigeminal ganglia (TG) were collected.

Plaque assay

Serially diluted viral samples were applied as inoculum onto monolayers of Vero cells plated in 24 well plates and plaques were counted as previously described [33].

Ocular toxicity evaluation

Ocular toxicity evaluation was conducted on fifteen 8-week-old male C57BL6 mice for 4 weeks. They were administered either 0.1% BAK, 10 µM BX795, or 50 µM TFT to the right eyes, while the left eyes were left non-treated. Toxicity evaluation was performed once per week under anesthesia.

Phenol red thread wetting: This assay was performed using a 30-mm-long phenol-red impregnated thread with 3-mm bent end that was placed in lower fornix of the mouse eye for 15 seconds. When the phenol red came in contact with alkaline tears, it changed color from yellow to red(40). The thread was removed after 15 seconds, and the length of the red portion was measured using a ruler. The results were interpreted as follows: wet length <2 mm as severe dry eye, ≤5 mm as borderline dry eye and >10 mm as normal tear production. Both treated and non-treated eyes were evaluated while the non-treated eye served as an internal control.

Slit-lamp biomicroscopic imaging: Anesthetized mice were placed on a sturdy mice holder and held in the right position such that the entire frame of the cornea was visible. Multiple images at 10X magnification were taken in quick succession to avoid drying of the eye using a slit-lamp biomicroscope (Haag-Streit AG, Koeniz, Switzerland) (41). Fluorescein (1%) dye was added in a total volume of 5 µL to each eye followed by manual blinking of the eye 5 times before images were captured in the GFP channel. The cornea was divided in 4 quadrants and each quadrant was scored in a double-blinded fashion to give a dryness score.

Optical coherence tomography (OCT): OCT images were taken on a Micron IV (Phoenix Technology group, CA, USA) with an OCT probe to specifically look at corneal thickness. Anesthetized mice were placed on a holder, and the OCT probe was brought closer to the eye. The light intensity, focus, angle and contrast were standardized on the first week of measurement. The same standard values were used throughout the entire course of the study. Once the images were captured, the epithelial, stromal, and total thickness of the cornea were measured for all the mice to evaluate the presence of inflammation. The results were interpreted as follows: <5% variation in thickness as normal, >5% and <10% as moderate inflammation, >10% as severe inflammation(42).

Esthesiometry: Corneal sensitivity of the mice eyes was measured by manual Esthesiometer (12/100 mm, LUNEAU SAS, France). Corneal sensitivity measurements as a function of blink response were conducted on wake mice. The nylon fiber of the esthesiometer was extended to the full length (6 cm), and the tip of the nylon thread was gently impressed to the center of the cornea. In a normal cornea, this should inflict a blink response which corresponds to a sensitivity score. If the mouse did not blink, the length of the nylon fiber was reduced by 0.5 cm, and the exercise was repeated until a blink response was observed. The results for this study were interpreted as follows: Score of 5.5 to 6 as normal, 5.5 to 3.5 as moderate loss of sensitivity, <3.5 as severe loss of corneal sensitivity(32).

Tonometry: The intraocular pressure (IOP) of mice was measured using a hand-held tonometer device which have been calibrated to measure the IOP specifically for murine models. The measurement of IOP was initially performed both on wake and anesthetized mice to understand the variation in values. Given that no variation was observed over 15 mice, we proceeded to take measurements on anesthetized mice for convenience purposes. A new tip was loaded into the tonometer for every sample group and calibrated prior to measurement. Each measurement was performed in triplicates to account for variability(43).

149 *Statistical Analysis*

150 Data was analyzed using GraphPad Prism version 6.01 for Windows (GraphPad Software, La Jolla, CA).
151 Measurements were tested for statistical significance using paired t-test. All tests were two-tailed, and
152 the threshold for statistical significance was defined as a $P \leq 0.05$.

153 **Results:**

154 *Effect of Prophylactic treatment with BX795 on HSV-1 infection in vitro*

155 To understand whether the use of BX795 as a prophylactic can confer protection from HSV-1 infection,
156 we treated HCEs for 24 hours prior to infection. During this period, no enhanced cell death was seen,
157 and the cells looked healthy. Post initial treatment, the drug was completely removed from the media,
158 washed with PBS twice, and HSV-1 was allowed to infect the cells (figure 1A). As positive controls, we
159 therapeutically added TFT and BX795 two hours post infection (figure 1B). To our surprise, BX795 pre-
160 treated cells looked healthy and were barely infected when observed 24 hours post infection. While
161 there was a small amount of virus detected in cells (figure 1D), robust efficacy was observed in cells that
162 were pre-treated with 10 µM BX795 for 24 hours (figure 1C). Furthermore, pre-treatment with BX795
163 was efficacious for a prolonged period post removal of the drug, extending up to 72 hours post
164 infection.

165 *BX795 pre-treated cells resist HSV-1 induced viral translation*

166 In order to determine the mechanism of prophylactic action we focused on potential blockage of host
167 Akt pathway by BX795[33]. HSV-1 induces the phosphorylation of protein kinase R (AKT) at serine 473 site
168 which results in the downstream phosphorylation of P70S6Kinase and the hyper-phosphorylation of the
169 EIF4E binding protein (4EBP1) at Threonine 37/46 sites causing the upregulation of viral protein
170 translation. For therapeutic action we showed previously that the addition of BX795 to HSV-1 infected

cells inhibits the hyper-phosphorylation of 4EBP1 and hence counters the virus's protein translational potential. In order to assess whether the prophylactic treatment with BX795 confers protection via this mechanism, we infected HCEs with 1 MOI of HSV-1 after prophylactically treating the cells for a period of 24 hours. The cells were lysed and immunoblotted 24 hours post infection to assess the phosphorylation status of AKT, P70S6K and 4EBP1 (Figure 2A). As expected, BX795 was able to significantly reduce HSV-1 induced phosphorylation of the aforementioned proteins and hence curbing the translation of viral proteins. This confirms that prophylactic treatment with BX795 can block virus induced protein translation even after removing the drug for a period of 24 hours. We hypothesize that prophylactic treatment with BX795 is able to inhibit AKT for a prolonged, yet in a reversible manner resulting in the loss of phosphorylation of the downstream components requisite for viral protein translation. This has been encased in a schematic shown in Figure 2C.

BX795 treatment of human corneal epithelial cells does not confer significant toxicity

In order to assess whether the addition of BX795 was causing toxicity issues which could indirectly relate to the antiviral efficacy, we performed a live cell PI imaging assay. BX795, DAPI (nuclear stain) and propidium iodide (PI-cell death marker) were added to cells for a period of 72 hours with intermittent images taken every 12 hours. Death occurring during this period could be recorded based on the number of cells taking up the PI stain. While there was a greater amount of cell death associated with cells treated with DMSO (figure 3A), the difference was non-significant and BX795 treated cells had death similar to those treated with TFT (figure 3B). In addition, an MTT assay to assess cell viability through mitochondrial activity was conducted. The results showed no significant difference in cell viability when compared to mock treated cells (figure 3C).

Topical prophylactic treatment with BX795 prior to murine ocular HSV-1 challenge

Given that we observed a robust protective effect of BX795 on corneal epithelial cells *in vitro*, we sought to test our hypothesis that prior treatment with BX795 can indeed protect murine corneas from a high titer HSV-1 infection. For this purpose, we administered either mock (DMSO), TFT (an FDA approved topical antiviral) or BX795 for a period of 24 hours prior to infecting murine corneas with a neurovirulent McKrae virus at a high titer ($5x10^5$ PFU). Ocular swabs taken on day 2 and day 4 revealed a significant reduction of infected mice virus in the BX795 pre-treated group similar to TFT control group (figure 4A and 4B). The DMSO treated mice had significantly higher amount of HSV-1 in the ocular washes and slowly developed ulcerative keratitis in the infected eye. Furthermore, to understand whether the HSV-1 infection quiescently travelled to the latent site of infection, the TG of the mice were extracted on day 7 post infection, and HSV-1 titers were quantified using a plaque assay (figure 4C). Surprisingly, while TFT treated murine TGs consisted of HSV-1 genomes, although in low quantities, BX795 treated TGs did not. This means that pre-treatment with BX795 not only confers protection of the cornea from apparent high doses of HSV-1 infection, it can even protect the mice from developing a latent HSV-1 infection.

Effect of topical BX795 on murine cornea

With the novel information that pre-treatment with BX795 can confer protection to murine corneas from highly virulent HSV-1 infection, we sought to understand whether its prolonged usage can cause any significant damage to the treated eye. Given that prophylactic treatments might last multiple days to weeks, murine eyes were dosed with either 10 µM BX795, 50 µM TFT, or DMSO thrice every day for 4 weeks continuously. During these weeks, the mice were carefully observed for any behavioural changes and weight loss. No noteworthy changes were observed by us or the staff veterinarian at the animal housing facility during the entire course of this study. One day prior to treatment and 7 days thereafter, the ocular toxicity studies were conducted on mice. The studies were done in this order; corneal sensitivity measurements on wake mice followed by sedation, tonometry measurements on sedated

mice, tear fluid measurement using phenol red thread test, epithelial damage assessment using fluorescein staining and slit lamp imaging, followed by OCT corneal thickness measurements.

Sustained treatment with topical BX795 does not affect corneal sensitivity and intraocular pressure

The sensitivity of the murine corneas was tested using a handheld esthesiometer. The measurements were performed on wake mice such that a blink response could be recorded in them by carefully touching the tip of the nylon thread to the centre of the cornea. In these studies, we observed no change in corneal sensitivity for murine corneas treated with TFT or BX795 over a period of 2 weeks. However, starting in the 3rd week, we started to observe a mild loss of corneal sensitivity in TFT and BX795 treated mice which was non-significant when compared to mock treated group. On the other hand, we observed a complete loss of corneal sensitivity within the first week of treatment in the BAK group. The intraocular pressure for TFT and BX795 treated groups did not change significantly over the course of 4 weeks. However, a significant increase in the IOP was measured for mice treated with BAK (figure 5B).

Topical administration of BX795 does not cause tear film loss or corneal dryness

Over the course of 4 weeks, we performed phenol red thread tear collection every week (figure 6A). No significant change in the length of tear fluid coloring was observed during this course for BX795 treated corneas when compared TFT treated corneas (figure 6B). On the other hand, corneas treated with BAK resulted in a significant loss of length in coloration of the phenol red thread while mock treated corneas showed almost negligible change in length of coloration. Given the acute corneal toxicity associated with BAK, we discontinued the treatment with BAK after 1 week of exposure.

Slit lamp imaging, which were done sequential to phenol red thread colouring, was performed to evaluate the dryness of the cornea through fluorescein staining (figure 6C). Here also, we did not

observe any significant differences in staining between the TFT treated and BX795 treated murine corneas. Although both groups were comparatively more stained than the non-treated corneas indicating that both TFT and BX795 indeed induce mild dryness to the murine corneas. However, the induction of dryness was not as acute as seen in the BAK treated mice (figure 6D). During the first two weeks of treatment, almost no difference between the mock treated and BX795 treated murine corneas were observed. Starting in the 3rd week, a slight increase in fluorescein staining and reduction in phenol read thread colouring length was observed. While the thread lengths were not short enough for us to treat them as dry eyes, the fluorescein stained eyes did not show dryness anywhere close to that of BAK.

Topical BX795 does not significantly alter corneal thickness

OCT measurements were performed on sedated mice after slit lamp imaging. The corneas were continuously hydrated using a balanced salt solution during the entire course of the measurement. From OCT measurements conducted on the murine corneas, we observed almost no change in the corneal structure for TFT and BX795 treated groups during the study (figure 7A). The corneas for BAK treated mice had their entire sub-corneal structures, epithelium, stroma and endothelium, completely amalgamated into a single large fibrous structure that could not be differentiated using an OCT image. In the contrary, no change in the sub-corneal structures were observed for mock, TFT and BX795 treated murine corneas. Thickness evaluation of these sub-corneal structures revealed a slight elevation in the stromal thickness for both TFT and BX795 treated corneas starting in the 3rd week of measurements. These observations are in-line with corneal sensitivity and dryness measurements which also show a slight elevation during this time period (figure 7B).

Discussion:

BX795 is a well-known TBK-1 inhibitor, which we showed last year to have excellent antiviral therapeutic activity against HSV-1 infection in the eye(32). In our previous study, we showed that BX795 generates

its therapeutic antiviral efficacy via specific suppression of hyperphosphorylation of 4EBP1 through the inhibition of PDK-1(32). In this study, we wanted to understand whether prophylactically treating corneas with topical administration of BX795 can prevent them from infection. Furthermore, we wanted to determine its corneal tolerability and safety. In this regard, we performed time course *in vitro* studies primarily to understand the effective duration and the mechanisms of a prophylactic treatment with BX795. If proven prophylactically efficacious and safe for prolonged ocular use, this drug could be taken by ocular HSV-1 patients who suffer from ACV resistant infections, especially given that HSV-1 does not have a commercial vaccine (44). We found that by using 10 µM concentrations of BX795, a 24 h pre-treatment period was enough to confer near complete protection to the cells. We hypothesized that this could be due to the inhibition of PDK-1 molecules that the virus requires for its translation. To test this hypothesis, we performed immunoblotting of BX795 pre-treated and HSV-1 infected corneal epithelial cells. As expected, we saw reduced phosphorylation of AKT, P70S6K and 4EBP1 hyper-phosphorylation in BX795 pre-treated samples compared to mock treated controls. It was also evident that HSV-1 was unable to translate early viral protein ICP0 in the pre-treated samples.

A unique feature of this study was to observe and analyse the ocular tolerability and toxicity of BX795 when used for a prolonged period of time. The most common side effect of topical drugs is the causation of dryness and related discomfort(45, 46). Our evaluation of corneal dryness for BX795 treated mice showed that there was no difference between the mock, TFT and BX795 treated groups for the first 2 weeks. However, a non-significant increase in dryness related fluorescein staining was observed starting 3rd week post treatment. The dryness did not worsen from 3rd to 4th week, indicating that toxicity associated with BX795 treatment was analogous to TFT and that neither of them had any acute toxicity associated with them at the therapeutic concentration.

283 The corneal sensitivity and intraocular pressure in the treatment groups did not change significantly
284 over a period of 4 weeks. However, a mild but non-significant decrease in sensitivity was observed in
285 both BX795 and TFT treated mice starting 3rd week post treatment, which did not worsen when checked
286 4 weeks post treatment. These results correspond with the mild dryness observed during the same
287 period, indicating that there may be some correlation between increase in ocular dryness and loss
288 corneal sensitivity by TFT and BX795 treatments. Along the same pattern, we observed a slight but non-
289 significant increase in stromal thickness starting 3rd week of treatment period. This indicates that there
290 might also be some amount of inflammation associated with these treatments. In the contrary, almost
291 no change in the intraocular pressure was observed during the entire course of the study for all
292 treatment groups. This suggests that the observations made with respect to dryness, loss of corneal
293 sensitivity, and OCT-related inflammation might be sub-clinical characteristics which might not play a
294 major role in corneal toxicity. Furthermore, readings taken one week after the last treatment dose
295 indicated a return to normalcy in all fronts (data not shown). These results show the clinical
296 translatability of BX795 especially in patients who suffer from ACV resistant infections. Our results are
297 very encouraging given that an effective vaccine against this ubiquitous virus has remained elusive to
298 the scientific world (44).

299 In conclusion, these results indicate that BX795 is not only effective in controlling HSV-1 infection in the
300 eye when treated therapeutically but also confers protection to the cornea when applied
301 prophylactically 24 hours prior to HSV-1 challenge. Corneal toxicity evaluation of BX795 revealed no
302 significant toxicity associated with the therapeutic concentration of 10 µM when dosed 3 times a day for
303 4 weeks when compared to the TFT treated group. Given that BX795 is an inhibitor of viral protein
304 synthesis that acts on the host translation machinery, we speculate that its activity would be relevant
305 not only for other herpesviral infections such as Cytomegalovirus (CMV) and herpes zoster (HZV), but

306 also for other DNA viruses such as human papilloma virus (HPV) and RNA viruses such as human
307 immunodeficiency virus (HIV).

308 *Acknowledgements:*

309 This work was supported by grants from the NIH (R01 EY024710, P30 EY001792) to D.S and NIH (K08
310 EY024339, R01 EY029409), VA (I01 BX004080) and DOD (W81XWH-17-1-0122) to VA. We also thank Dr.
311 Arun Balasubramaniam, Ruth Zelkha and Tara Nguyen for their help and training with OCT and the tear
312 production test.

313 *Author contributions:*

314 T.Y., V.A., and D.S. designed the experiments. T.Y., R.S., M.A., A.Q., and R.K. performed *in vitro*
315 experiments. T.Y., R.S., A.Q., J.A., and M.A. performed *in vivo* experiments. T.Y., R.K., and D.S. wrote the
316 manuscript.

1. **Coleman, J. L., and D. Shukla.** 2013. Recent advances in vaccine development for herpes simplex virus types i and II. Hum. Vaccines Immunother. **9:**729-735. doi: 10.4161/hv.23289. https://www.scopus.com/inward/record.uri?eid=2-s2.0-84877138314&partnerID=40&md5=794fd7792e6dcc452c873dc01e86a729.

2. **Farooq, A. V., T. Valyi-Nagy, and D. Shukla.** 2010. Mediators and mechanisms of herpes simplex virus entry into ocular cells. Curr. Eye Res. **35:**445-450. doi: 10.3109/02713681003734841. https://www.scopus.com/inward/record.uri?eid=2-s2.0-77952482928&partnerID=40&md5=b5d106681dd529315705c5713b81931f.

3. **Whitley, R. J., and B. Roizman.** 2001. Herpes simplex virus infections. Lancet. **357:**1513-1518. https://www.scopus.com/inward/record.uri?eid=2-s2.0-0035849323&doi=10.1016%2fS0140-6736%2800%2904638-9&partnerID=40&md5=04ca89a33775aa023e41da57797a589b.

4. **Shah, A., A. V. Farooq, V. Tiwari, M. Kim, and D. Shukla.** 2010. HSV-1 infection of human corneal epithelial cells: receptor-mediated entry and trends of re-infection. Molecular Vision. **16:**2476-2486. https://www.ncbi.nlm.nih.gov/pubmed/21139972.

5. **Yakoub, A. M., and D. Shukla.** 2015. Herpes Simplex Virus-1 Fine-Tunes Host's Autophagic Response to Infection: A Comprehensive Analysis in Productive Infection Models. PloS One. **10:**e0124646. doi: 10.1371/journal.pone.0124646. https://www.ncbi.nlm.nih.gov/pubmed/25894397.

6. **Thomas, J., and B. T. Rouse.** 1997. Immunopathogenesis of herpetic ocular disease. Immunol. Res. **16:**375-386. https://www.scopus.com/inward/record.uri?eid=2-s2.0-0031439721&doi=10.1007%2fBF02786400&partnerID=40&md5=b13b1d032410387d201a6950fa24e41e.

7. **Looker, K. J., A. S. Magaret, M. T. May, K. M. E. Turner, P. Vickerman, S. L. Gottlieb, and L. M. Newman.** 2015. Global and regional estimates of prevalent and incident herpes simplex virus type 1 infections in 2012. PLoS ONE. **10:**. https://www.scopus.com/inward/record.uri?eid=2-s2.0-84950133180&doi=10.1371%2fjournal.pone.0140765&partnerID=40&md5=df6dfcf60da6c3434567bdb5f11e7a0c.

8. **Agelidis, A. M., and D. Shukla.** 2015. Cell entry mechanisms of HSV: what we have learned in recent years. Future Virology. **10:**1145-1154. doi: 10.2217/fvl.15.85. http://dx.doi.org/10.2217/fvl.15.85.

9. **Jaishankar, D., and D. Shukla.** 2016. Genital Herpes: Insights into Sexually Transmitted Infectious Disease. Microbial Cell (Graz, Austria). **3:**438-449. doi: 10.15698/mic2016.09.528. https://www.ncbi.nlm.nih.gov/pubmed/28357380.

10. **Mishra, Y. K., R. Adelung, C. Röhl, D. Shukla, F. Spors, and V. Tiwari.** 2011. Virostatic potential of micro–nano filopodia-like ZnO structures against herpes simplex virus-1. Antiviral Research. **92:**305-312. doi: 10.1016/j.antiviral.2011.08.017. https://www.sciencedirect.com/science/article/pii/S0166354211004189.

11. **Jaggi, U., S. Wang, K. Tormanen, H. Matundan, A. V. Ljubimov, and H. Ghiasi.** 2018. Role of Herpes Simplex Virus Type 1 (HSV-1) Glycoprotein K (gK) Pathogenic CD8+ T Cells in Exacerbation of Eye Disease. Front Immunol. **9:**2895. doi: 10.3389/fimmu.2018.02895.

12. **Smith, J. S., and N. J. Robinson.** 2002. Age-Specific Prevalence of Infection with Herpes Simplex Virus Types 2 and 1: A Global Review. J Infect Dis. **186:**S-S28. doi: 10.1086/343739. https://academic.oup.com/jid/article/186/Supplement_1/S3/836780.

13. **Lobo, A. -., A. M. Agelidis, and D. Shukla.** 2019. Pathogenesis of herpes simplex keratitis: The host cell response and ocular surface sequelae to infection and inflammation. Ocular Surface. **17:**40-49. https://www.scopus.com/inward/record.uri?eid=2-s2.0-85055085351&doi=10.1016%2fj.jtos.2018.10.002&partnerID=40&md5=32987500b4168bab976dd157696e7afc.

14. **Wald, A., and L. Corey.** 2007. Persistence in the population: epidemiology, transmission*In* A. Arvin, G. Campadelli-Fiume, E. Mocarski, P. S. Moore, B. Roizman, R. Whitley, and K. Yamanishi (eds.), Human Herpesviruses: Biology, Therapy, and Immunoprophylaxis. Cambridge University Press, Cambridge. http://www.ncbi.nlm.nih.gov/books/NBK47447/.

15. **Yadavalli, T., A. Agelidis, D. Jaishankar, K. Mangano, N. Thakkar, K. Penmetcha, and D. Shukla.** 2017. Targeting Herpes Simplex Virus-1 gD by a DNA Aptamer Can Be an Effective New Strategy to Curb Viral Infection. Molecular Therapy - Nucleic Acids. **9:**365-378. doi: 10.1016/j.omtn.2017.10.009. https://www.sciencedirect.com/science/article/pii/S2162253117302706.

16. **Patel, A., K. Cholkar, V. Agrahari, and A. K. Mitra.** 2013. Ocular drug delivery systems: An overview. World Journal of Pharmacology. **2:**47. doi: 10.5497/wjp.v2.i2.47. https://www.ncbi.nlm.nih.gov/pubmed/25590022.

17. **Suwannoi, P., M. Chomnawang, A. Tunsirikongkon, A. Phongphisutthinan, C. C. Müller-Goymann, and N. Sarisuta.** 2019. TAT-surface modified acyclovir-loaded albumin nanoparticles as a novel ocular drug delivery system. Journal of Drug Delivery Science and Technology. **52:**624-631. doi: 10.1016/j.jddst.2019.05.029. https://www.sciencedirect.com/science/article/pii/S1773224718314965.

18. **Tsatsos, M., C. MacGregor, I. Athanasiadis, M. M. Moschos, P. Hossain, and D. Anderson.** 2016. Herpes simplex virus keratitis: an update of the pathogenesis and current treatment with oral and topical antiviral agents. Clinical & Experimental Ophthalmology. **44:**824-837. doi: 10.1111/ceo.12785. https://onlinelibrary.wiley.com/doi/abs/10.1111/ceo.12785.

19. **Elion, G. B.** 1993. Acyclovir: Discovery, mechanism of action, and selectivity. Journal of Medical Virology. **41:**2-6. doi: 10.1002/jmv.1890410503. https://onlinelibrary.wiley.com/doi/abs/10.1002/jmv.1890410503.

20. **Chemaly, R. F., J. A. Hill, S. Voigt, and K. S. Peggs.** 2019. In vitro comparison of currently available and investigational antiviral agents against pathogenic human double-stranded DNA viruses: A systematic literature review. Antiviral Research. **163:**50-58. doi: 10.1016/j.antiviral.2019.01.008. https://www.sciencedirect.com/science/article/pii/S0166354218306570.

21. **Andrei, G., and R. Snoeck.** 2013. Herpes simplex virus drug-resistance: new mutations and insights. Current Opinion in Infectious Diseases. **26:**551-560. doi: 10.1097/QCO.0000000000000015. insights.ovid.com.

22. **Chilukuri, S., and T. Rosen.** 2003. Management of acyclovir-resistant herpes simplex virus. Dermatologic Clinics. **21:**311-320. doi: 10.1016/S0733-8635(02)00093-1. https://www.sciencedirect.com/science/article/pii/S0733863502000931.

23. **Koujah, L., R. K. Suryawanshi, and D. Shukla.** 2019. Pathological processes activated by herpes simplex virus-1 (HSV-1) infection in the cornea. Cellular and Molecular Life Sciences. **76:**405-419. https://www.scopus.com/inward/record.uri?eid=2-s2.0-85055469633&doi=10.1007%2fs00018-018-2938-1&partnerID=40&md5=f90e930afbfe2b42c76ca09836a2bc54.

24. **Yu-Chen Jiang Hui Feng Yu-Chun Lin Xiu-Rong Guo.** 2016. New strategies against drug resistance to herpes simplex virus. 国际口腔科学杂志：英文版. **8:**1-6. doi: 10.1038/ijos.2016.3. http://lib.cqvip.com/qk/89520X/201601/668656637.html.

25. **Larder, B. A., Y. Cheng, and G. Darby.** 1983. Characterization of Abnormal Thymidine Kinases Induced by Drug-resistant Strains of Herpes Simplex Virus Type 1. Journal of General Virology. **64:**523-532. doi: 10.1099/0022-1317-64-3-523. https://jgv.microbiologyresearch.org/content/journal/jgv/10.1099/0022-1317-64-3-523.

26. **Strick, L. B., A. Wald, and C. Celum.** 2006. Management of Herpes Simplex Virus Type 2 Infection in HIV Type 1–Infected Persons. Clin Infect Dis. **43:**347-356. doi: 10.1086/505496. https://academic.oup.com/cid/article/43/3/347/333493.

27. **Jaishankar, D., A. M. Yakoub, A. Bogdanov, T. Valyi-Nagy, and D. Shukla.** 2015. Characterization of a proteolytically stable D-peptide that suppresses herpes simplex virus 1 infection: Implications for the development of entry-based antiviral therapy. J. Virol. **89:**1932-1938. doi: 10.1128/JVI.02979-14. https://www.scopus.com/inward/record.uri?eid=2-s2.0-84921468650&partnerID=40&md5=66b92beffe489d7a020caaad90b867bb.

28. **Jaishankar, D., J. S. Buhrman, T. Valyi-Nagy, R. A. Gemeinhart, and D. Shukla.** 2016. Extended release of an anti–heparan sulfate peptide from a contact lens suppresses corneal herpes simplex virus-1 infection. Invest. Ophthalmol. Visual Sci. **57:**169-180. https://www.scopus.com/inward/record.uri?eid=2-s2.0-84955296050&doi=10.1167%2fiovs.15-18365&partnerID=40&md5=b863c8f19c425cf8eab6635273082f71.

29. **Agelidis, A., L. Koujah, R. Suryawanshi, T. Yadavalli, Y. K. Mishra, R. Adelung, and D. Shukla.** 2019. An intra-vaginal zinc oxide tetrapod nanoparticles (zoten) and genital herpesvirus cocktail can provide a novel platform for live virus vaccine. Frontiers in Immunology. **10:**. https://www.scopus.com/inward/record.uri?eid=2-s2.0-85064326244&doi=10.3389%2ffimmu.2019.00500&partnerID=40&md5=814bcba00e060268ac54cb6a367e9ce6.

30. **Yadavalli, T., and D. Shukla.** 2017. Role of metal and metal oxide nanoparticles as diagnostic and therapeutic tools for highly prevalent viral infections. Nanomed. Nanotechnol. Biol. Med. **13:**219-230.

427 doi: 10.1016/j.nano.2016.08.016. https://www.scopus.com/inward/record.uri?eid=2-s2.0-
428 84997785112&doi=10.1016%2fj.nano.2016.08.016&partnerID=40&md5=489acaf4d34809f24a94431853
429 22434b.

430 31. **Yadavalli, T., J. Ames, A. Agelidis, R. Suryawanshi, D. Jaishankar, J. Hopkins, N. Thakkar, L. Koujah,**
431 **and D. Shukla.** 2019. Drug-encapsulated carbon (DECON): A novel platform for enhanced drug delivery.
432 Sci Adv. **5:**eaax0780. doi: 10.1126/sciadv.aax0780.
433 http://advances.sciencemag.org/content/5/8/eaax0780.abstract.

434 32. **Jaishankar, D., A. M. Yakoub, T. Yadavalli, A. Agelidis, N. Thakkar, S. Hadigal, J. Ames, and D.**
435 **Shukla.** 2018. An off-target effect of BX795 blocks herpes simplex virus type 1 infection of the eye. Sci.
436 Transl. Med. **10:**. doi: 10.1126/scitranslmed.aan5861.
437 https://www.scopus.com/inward/record.uri?eid=2-s2.0-
438 85042067967&doi=10.1126%2fscitranslmed.aan5861&partnerID=40&md5=6aaa577196c26eb78ac4631
439 e0b7d6588.

440 33. **Clark, K., L. Plater, M. Peggie, and P. Cohen.** 2009. Use of the Pharmacological Inhibitor BX795 to
441 Study the Regulation and Physiological Roles of TBK1 and IκB Kinase ϵ. Journal of Biological Chemistry.
442 **284:**14136-14146. doi: 10.1074/jbc.M109.000414. http://www.jbc.org/content/284/21/14136.

443 34. **Williams, L. E., A. B. Nesburn, and H. E. Kaufman.** 1965. EXPERIMENTAL INDUCTION OF DISCIFORM
444 KERATITIS. Arch. Ophthalmol. **73:**112-114. doi: 10.1001/archopht.1965.00970030114023.

445 35. **Macdonald, S. J., H. H. Mostafa, L. A. Morrison, and D. J. Davido.** 2012. Genome sequence of herpes
446 simplex virus 1 strain McKrae. J. Virol. **86:**9540-9541. doi: 10.1128/JVI.01469-12.

447 36. **Brown, S. M., D. A. Ritchie, and J. H. Subak-Sharpe.** 1973. Genetic studies with herpes simplex virus
448 type 1. The isolation of temperature-sensitive mutants, their arrangement into complementation groups
449 and recombination analysis leading to a linkage map. J. Gen. Virol. **18:**329-346. doi: 10.1099/0022-1317-
450 18-3-329.

451 37. **Desai, P., and S. Person.** 1998. Incorporation of the green fluorescent protein into the herpes
452 simplex virus type 1 capsid. J. Virol. **72:**7563-7568.

453 38. **Pereira, S. R., M. A. Guimarães, L. V. Neto, D. Segenreich, R. B. Varella, V. L. Antunes Chagas, and F.**
454 **P. Câmara.** 2001. Herpes simplex virus ophthalmic disease induced using two different methods of mice
455 inoculation. The Brazilian Journal of Infectious Diseases : An Official Publication of the Brazilian Society
456 of Infectious Diseases. **5:**183-191. doi: 10.1590/S1413-86702001000400004.
457 https://www.ncbi.nlm.nih.gov/pubmed/11712963.

458 39. **BenMohamed, L., N. Osorio, A. A. Khan, R. Srivastava, L. Huang, J. J. Krochmal, J. M. Garcia, J. L.**
459 **Simpson, and S. L. Wechsler.** 2016. Prior Corneal Scarification and Injection of Immune Serum are Not
460 Required Before Ocular HSV-1 Infection for UV-B-Induced Virus Reactivation and Recurrent Herpetic
461 Corneal Disease in Latently Infected Mice. Curr Eye Res. **41:**747-756. doi:
462 10.3109/02713683.2015.1061024. https://www.ncbi.nlm.nih.gov/pmc/articles/PMC5349863/.

40. **Kilic, S., and K. Kulualp.** 2016. Tear production rate in a mouse model of dry eye according to the phenol red thread and endodontic absorbent paper point tear tests. Comp. Med. **66:**367-372. https://www.scopus.com/inward/record.uri?eid=2-s2.0-84991717356&partnerID=40&md5=2139369267c35ce2d1aae434768a0de9.

41. **Kim, C., D. Barbut, M. H. Heinemann, G. Pasternak, and M. I. Rosenblatt.** 2014. Synthetic neurotensin analogues are nontoxic analgesics for the rabbit cornea. Invest. Ophthalmol. Vis. Sci. **55:**3586-3593. doi: 10.1167/iovs.13-13050. https://www.scopus.com/inward/record.uri?eid=2-s2.0-84902449006&doi=10.1167%2fiovs.13-13050&partnerID=40&md5=64afb97082af3754f7e2ed36b7f33978.

42. **Igbre, A. O., M. C. Rico, and S. J. Garg.** 2014. High-speed optical coherence tomography as a reliable adjuvant tool to grade ocular anterior chamber inflammation. Retina. **34:**504-508. doi: 10.1097/IAE.0b013e31829f73bd. https://www.scopus.com/inward/record.uri?eid=2-s2.0-84894465758&doi=10.1097%2fIAE.0b013e31829f73bd&partnerID=40&md5=297bc1a1cf75b3efd32ad358cfcaa24d.

43. **Fan, Y., L. Guo, J. Wei, J. Chen, H. Sun, and T. Guo.** 2019. Effects of salidroside on trabecular meshwork cell extracellular matrix expression and mouse intraocular pressure. Invest. Ophthalmol. Vis. Sci. **60:**2072-2082. doi: 10.1167/iovs.19-26585. https://www.scopus.com/inward/record.uri?eid=2-s2.0-85066858865&doi=10.1167%2fiovs.19-26585&partnerID=40&md5=6d4846be7338735284ed907ee02cb55c.

44. **Koelle, D. M., and H. Ghiasi.** 2005. Prospects for developing an effective vaccine against ocular herpes simplex virus infection. Curr. Eye Res. **30:**929-942. doi: 10.1080/02713680500313153.

45. **Boddu, S. H. S., and Patel, Himanshu Gupta and Soohi.** 2014. Drug Delivery to the Back of the Eye Following Topical Administration: An Update on Research and Patenting Activity. **2019:**10. http://www.eurekaselect.com/120034/article.

46. **Cholkar, K., A. D. Vadlapudi, H. M. Trinh, and A. K. Mitra.** 2014. Compositions, formulation, pharmacology, pharmacokinetics, and toxicity of topical, periocular, and intravitreal ophthalmic drugs. Methods in Pharmacology and Toxicology. 91-118. doi: 10.1007/7653-2013-10.

47. **Lemp, M. A.** 1995. Report of the National Eye Institute/Industry Workshop on Clinical Trials in Dry Eyes. Clao J. **21:**221-232. https://www.scopus.com/inward/record.uri?eid=2-s2.0-0028849933&partnerID=40&md5=eedcda0053668e07b51fdd77f9b54950.

Figure 1: Prophylactic treatment with BX795 protects corneal cells from HSV-1 infection. (A) Schematic showing the method of treatment used in this study. Human corneal epithelial cells were pre-treated with either BX795 (10 μM) or TFT (50 μM) for 24 hours followed by the addition of HSV-1 17 GFP virus for 72 hours. (B) As a control to assess the known efficacy of the drugs, infected cells were therapeutically treated 2 hours post infection. (C) At noted time points, infected cells were imaged for the presence of virus (green) and collected for titration using a plaque assay (D). Two-way ANOVA with Dunnett's multiple comparison test, ****$p < 0.0001$ was conducted (n=3 replicates).

Figure 2: Cells pre-treated with BX795 resist HSV-1 induced viral translation. (A) HCEs were either prophylactically treated with BX795 or mock for a period of 24 hours prior to infection with mock or HSV-1 at 1 MOI. At 24 hours post infection, cells were lysed and immunoblotted for suggested proteins. (B) The quantification of the immunoblots for phospho-proteins relative to their total proteins and normalized to GAPDH values. HSV-1 proteins gD and ICP0 were normalized to GAPDH. Unpaired student's t-test was conducted to compare the relative blot intensities of HSV-1 infected cells either mock or BX795 pre-treated. *$p < 0.05$, **$p < 0.01$. (C) A schematic explaining the probable mechanism of action through which BX795 is able to inhibit HSV-1 protein translation.

Figure 3: BX795 treatment does not cause significant cell death. (A) HCEs were stained with propidium iodide (PI-cell death marker) and DAPI (nuclear stain) prior to the addition of either DMSO, TFT (50 μM) or BX795 (10 μM). The cells were imaged at shown time points to assess the extent of PI taken up by cells (a mark of death). (B) Total number of cells (DAPI) present and number cells with PI stain in 4 frames were counted and averaged over 3 replicates. The graph represents the percent of dead cells (stained with PI) over a period of 72 hours. Two-way ANOVA with Dunnett's multiple comparison test, $p < 0.05$ was conducted (n=3 replicates).

Figure 4: BX795 pre-treatment protects mice from ocular HSV-1 infection. (A) Schematic of the experiment. Ocular surface of C57BL/6 mice were dosed (n=5) with either Mock, TFT or BX795 3 times within a time frame of 24 hours prior to infection with HSV-1 McKrae ($5x10^5$ PFU). (B) On day 2 and day 4 post infection, ocular swabs were collected from these mice and overlaid on Vero cells to quantify shed virus via a plaque assay. (C) The trigeminal ganglia from these mice were harvested and overlaid on Vero cells to quantify latent site infection. Significance was calculated by one-way ANOVA using a Dunnet's multiple comparison test*$p<0.05$, **$p<0.01$.

Figure 5: No significant change to corneal sensitivity and intraocular pressure were observed with BX795 treatment. Over a period of 4 weeks, either BX795 or TFT were added 3 times every day. (A) Every 7 days, the corneal sensitivity was measured via an esthesiometer on wake mice. Lower values correspond to loss of corneal sensitivity. (B) Mice were anesthetized and the IOP was measured using a murine specific tonometer. Higher values indicate an increase in the IOP of the mice. Two-way ANOVA with Dunnett's multiple comparison test, $p < 0.05$ was conducted (n=5 replicates).

Figure 6: Treatment with BX795 does not cause loss of tear film or damage to the corneal epithelium. Eyes of anesthetized mice were probed with a phenol red thread to assess the extent of wettability of the tear fluid. (A) Upon contact with the phenol read thread, tears cause a change in the coloration from light yellow to dark red. Greater wetting length directly correspond to higher tearing ability of the eye. (B) A graph detailing the percentage decline in wetting length over a period of 4 weeks for all the sample groups. Two-way ANOVA with Dunnett's multiple comparison test, **** $p < 0.0001$ was conducted (n=5 replicates). (C) Anesthetized mice were placed on a holder and a slit lamp instrument was used to capture the picture of the corneal surface. (D) The eyes were then stained with fluorescein to identify fault zones across the corneal surface. Increased fluorescein staining corresponds to greater damage to the corneal surface. (E) Fluorescein stained images of the murine corneas were shown to reviewers who

were blind to the study. Dryness scores were given using the Corneal Fluorescein Score of the National Eye Institute after segmenting the ocular image into 5 quadrants(47). The scores were summed up and then plotted to visualize the change in dryness scores over a period of 3 weeks. Two-way ANOVA with Dunnett's multiple comparison test was conducted while comparing score means per week within each group. ***p<0.001, ****p<0.0001.

Figure 7: No inflammation associated increase in corneal thickness is observed in BX795 treated eyes. (A) Anesthetized mice were placed on a stand and their eyes were help open in contact with the Micron IV OCT instrument. The focus dials were adjusted to bring the corneal layer into view and images were taken. (B) A graph representing the epithelial, stromal and total thickness of the cornea pre and post 4 weeks of either BX795 or TFT treatment. Two-way ANOVA with Dunnett's multiple comparison test, *** $p < 0.001$ was conducted (n=5 replicates).

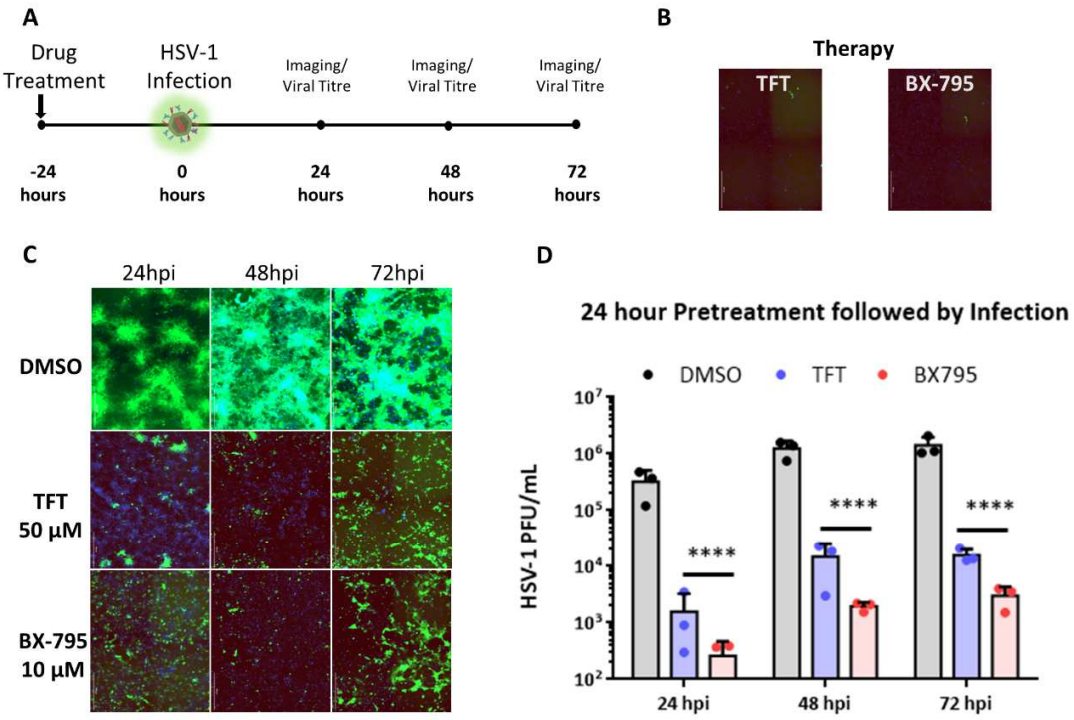

Figure 1: Prophylactic treatment with BX795 protects corneal cells from HSV-1 infection. (A) Schematic showing the method of treatment used in this study. Human corneal epithelial cells were pre-treated with either BX795 (10 µM) or TFT (50 µM) for 24 hours followed by the addition of fresh media with HSV-1 17 GFP virus for 72 hours. (B) As a control to assess the known efficacy of the drugs, infected cells were therapeutically treated 2 hours post infection. (C) At noted time points, infected cells were imaged for the presence of virus (green) and collected for titration using a plaque assay (D). Two-way ANOVA with Dunnett's multiple comparison test, ****$p < 0.0001$ was conducted (n=3 replicates).

553

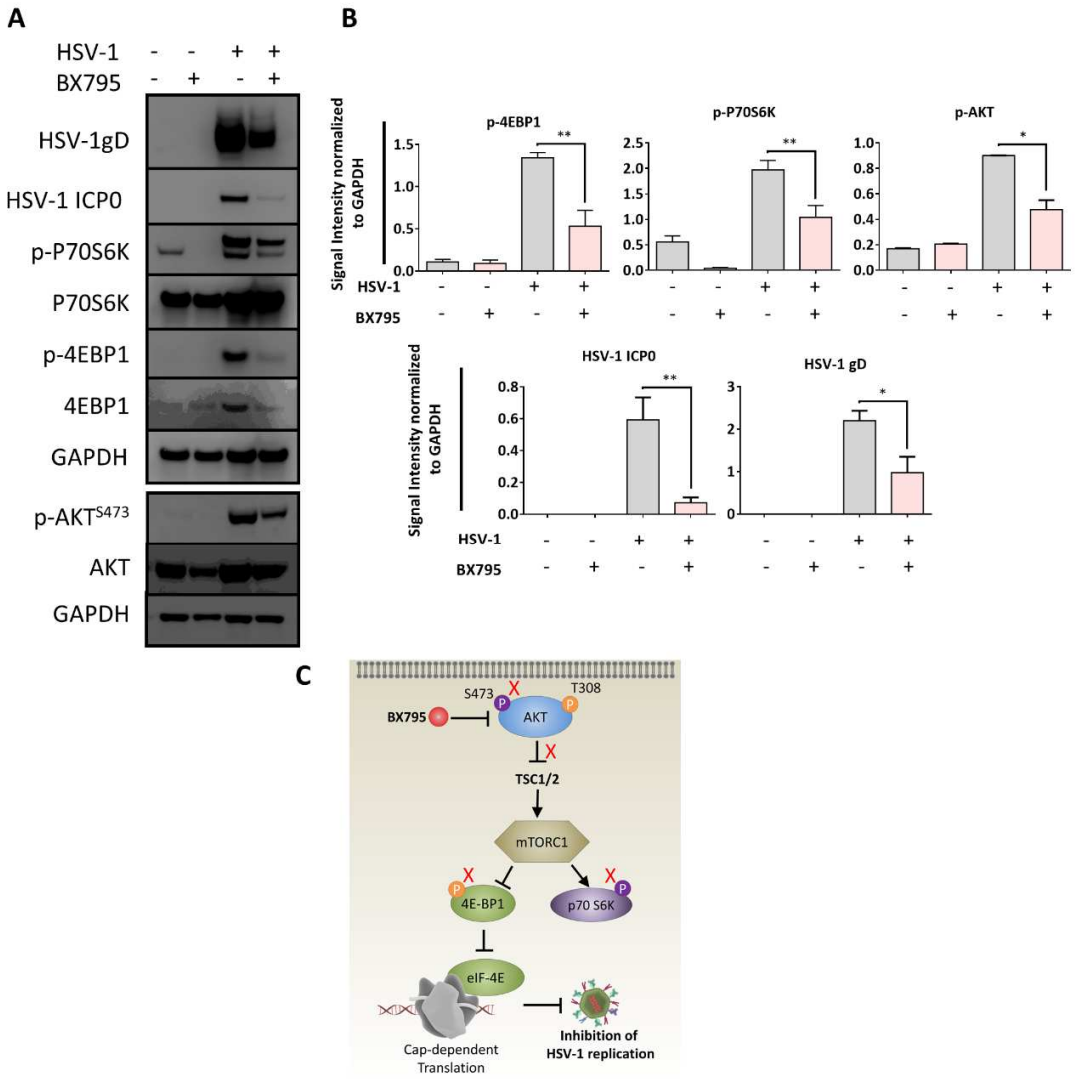

Figure 2: Cells pre-treated with BX795 resist HSV-1 induced viral translation. (A) HCEs were either prophylactically treated with BX795 or mock for a period of 24 hours prior to infection with mock or HSV-1 at 1 MOI. At 24 hours post infection, cells were lysed and immunoblotted for suggested proteins. (B) The quantification of the immunoblots for phospho-proteins relative to their total proteins and normalized to GAPDH values. HSV-1 proteins gD and ICP0 were normalized to GAPDH. Unpaired student's t-test was conducted to compare the relative blot intensities of HSV-1 infected cells either mock or BX795 pre-treated. *$p < 0.05$, **$p < 0.01$. (C) A schematic explaining the probable mechanism of action through which BX795 is able to inhibit HSV-1 protein translation.

554

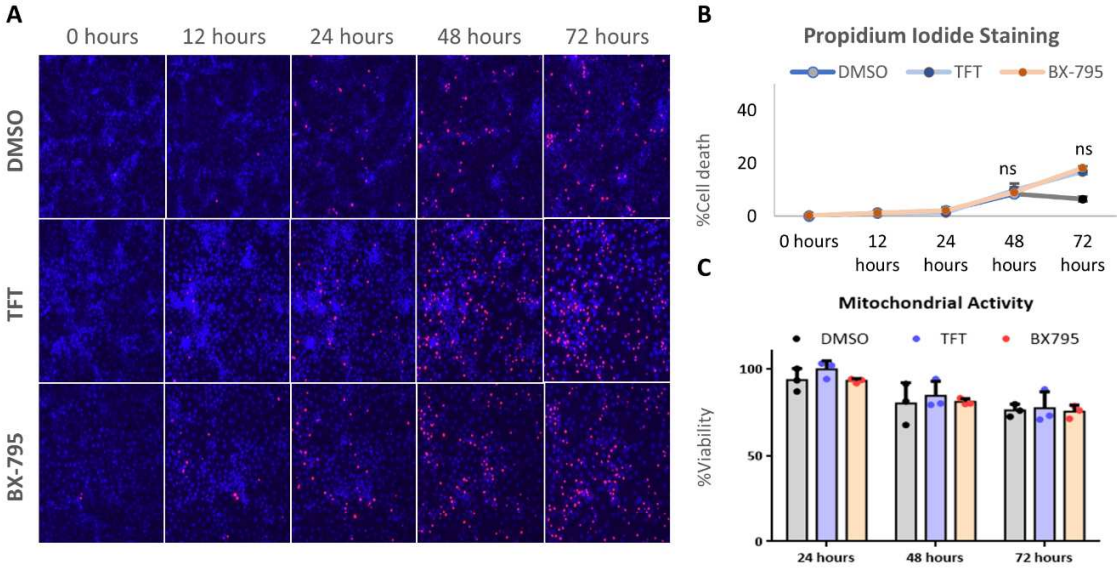

Figure 3: BX795 treatment does not cause significant cell death. (A) HCEs were stained with propidium iodide (PI-cell death marker) and DAPI (nuclear stain) prior to the addition of either DMSO, TFT (50 µM) or BX795 (10 µM). The cells were imaged at shown time points to assess the extent of PI taken up by cells (a mark of death). (B) Total number of cells (DAPI) present and number cells with PI stain in 4 frames were counted and averaged over 3 replicates. The graph represents the percent of dead cells (stained with PI) over a period of 72 hours. Two-way ANOVA with Dunnett's multiple comparison test, $p < 0.05$ was conducted (n=3 replicates).

555

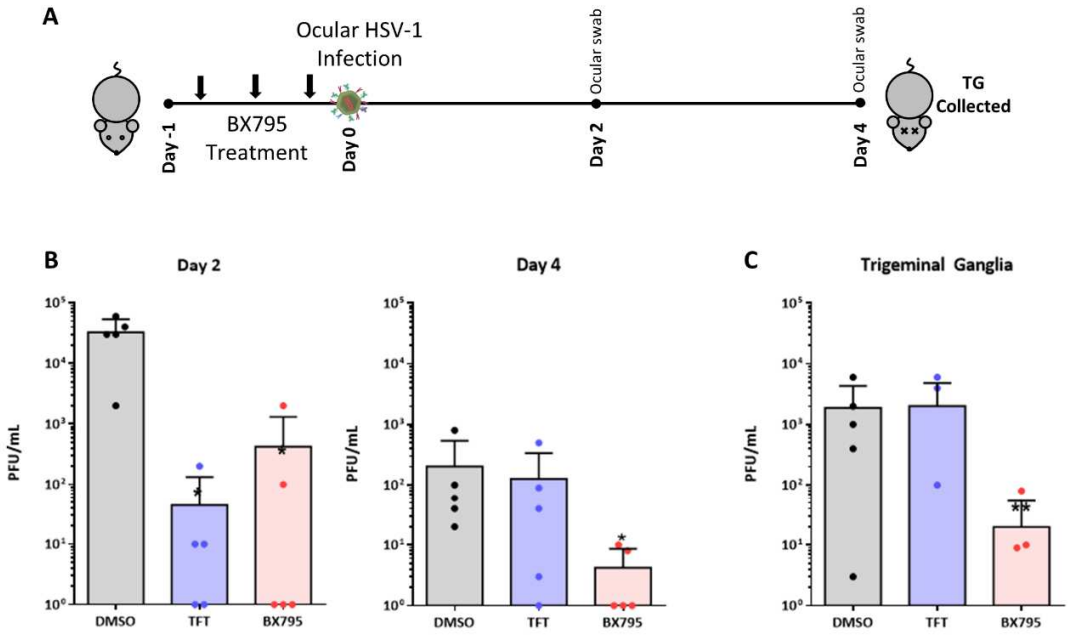

Figure 4: BX795 pre-treatment protects mice from ocular HSV-1 infection. (A) Schematic of the experiment. Ocular surface of C57BL/6 mice were dosed (n=5) with either Mock, TFT or BX795 3 times within a time frame of 24 hours prior to infection with HSV-1 McKrae ($5x10^5$ PFU). (B) On day 2 and day 4 post infection, ocular swabs were collected from these mice and overlaid on Vero cells to quantify shed virus via a plaque assay. (C) The trigeminal ganglia from these mice were harvested and overlaid on Vero cells to quantify latent site infection. Significance was calculated by one-way ANOVA using a Dunnet's multiple comparison test*$p<0.05$, **$p<0.01$.

556

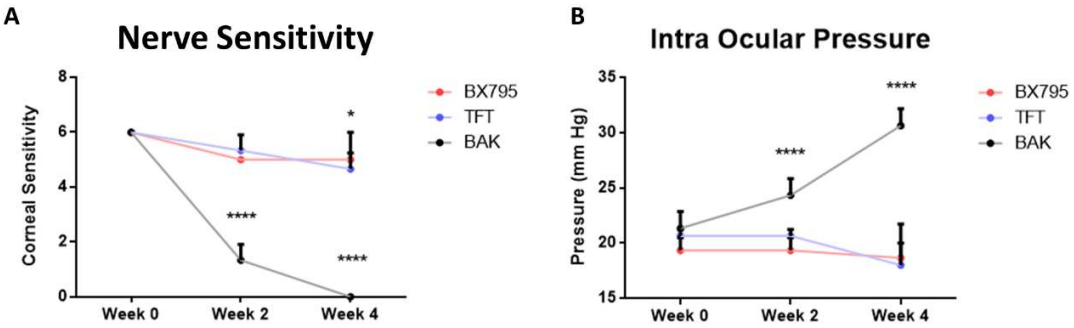

Figure 5: No significant change to corneal sensitivity and intraocular pressure were observed with BX795 treatment. Over a period of 4 weeks, either BX795 or TFT were added 3 times every day. (A) Every 7 days, the corneal sensitivity was measured via an esthesiometer on wake mice. Lower values correspond to loss of corneal sensitivity. (B) Mice were anesthetized and the IOP was measured using a murine specific tonometer. Higher values indicate an increase in the IOP of the mice. Two-way ANOVA with Dunnett's multiple comparison test, $p < 0.05$ was conducted (n=5 replicates).

557

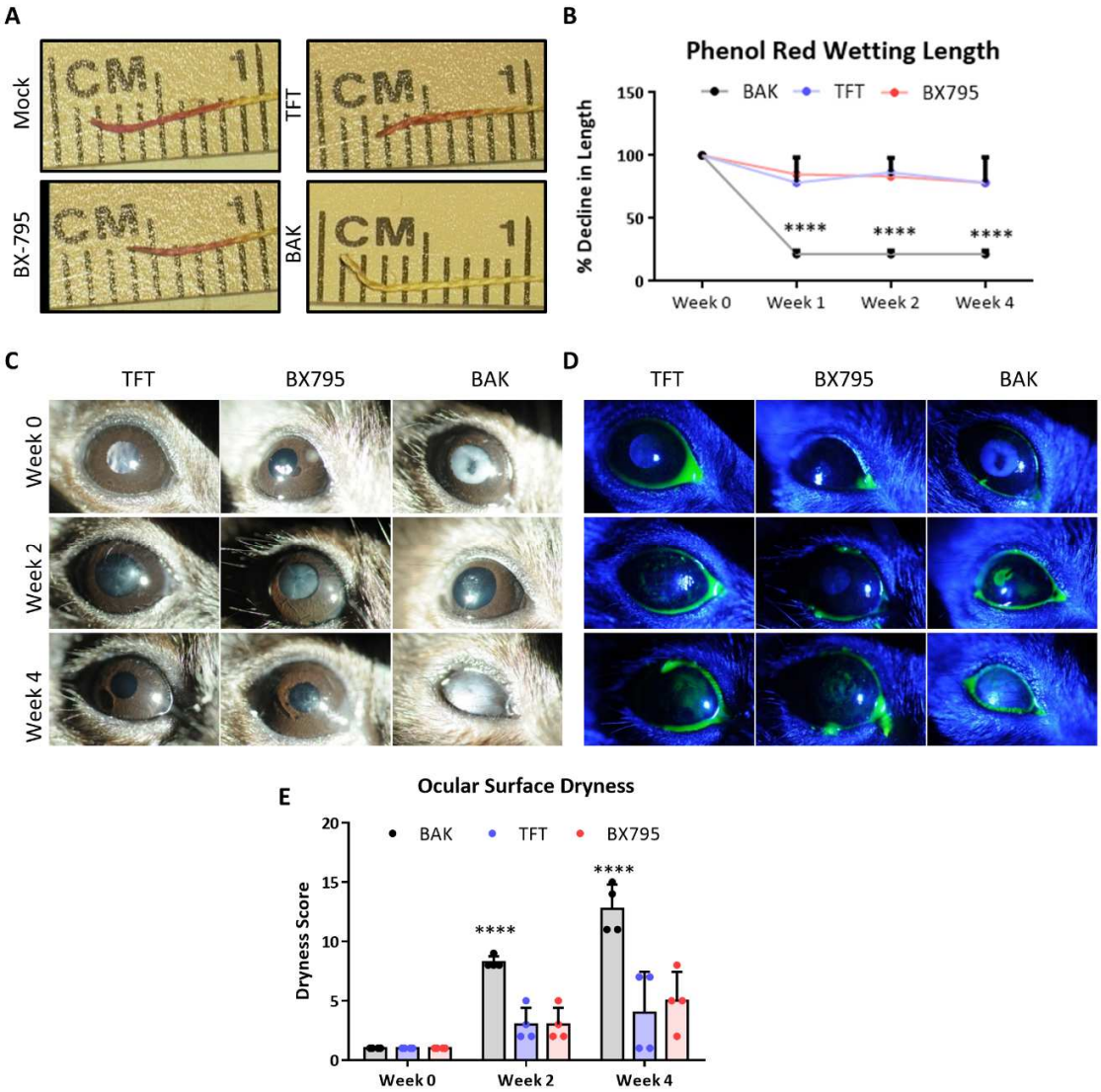

Figure 6: Treatment with BX795 does not cause loss of tear film or damage to the corneal epithelium. Eyes of anesthetized mice were probed with a phenol red thread to assess the extent of wettability of the tear fluid. (A) Upon contact with the phenol read thread, tears cause a change in the coloration from light yellow to dark red. Greater wetting length directly correspond to higher tearing ability of the eye. (B) A graph detailing the percentage decline in wetting length over a period of 4 weeks for all the sample groups. Two-way ANOVA with Dunnett's multiple comparison test, **** $p < 0.0001$ was conducted (n=5 replicates). (C) Anesthetized mice were placed on a holder and a slit lamp instrument was used to capture the picture of the corneal surface. (D) The eyes were then stained with fluorescein to identify fault zones across the corneal surface. Increased fluorescein staining corresponds to greater damage to the corneal surface. (E) Fluorescein stained images of the murine corneas were shown to reviewers who were blind to the study. Dryness scores were given using the Corneal Fluorescein Score of the National Eye Institute after segmenting the ocular image into 5 quadrants[39]. The scores were summed up and then plotted to visualize the change in dryness scores over a period of 3 weeks. Two-way ANOVA with Dunnett's multiple comparison test was conducted while comparing score means per week within each group. ***p<0.001, ****p<0.0001.

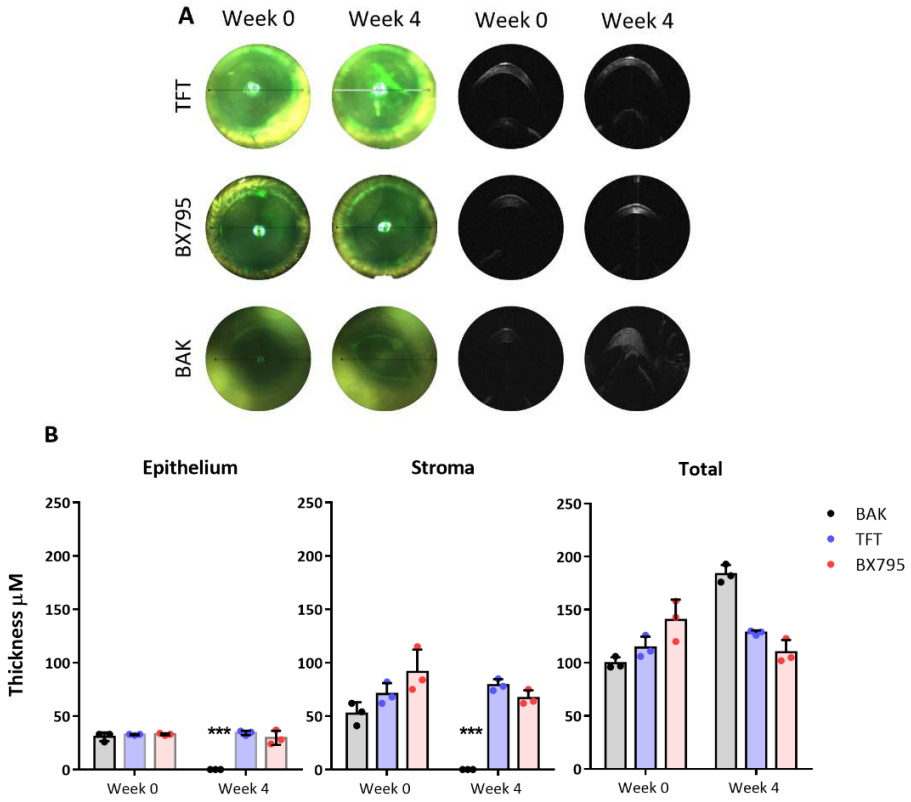

Figure 7: No inflammation associated increase in corneal thickness is observed in BX795 treated eyes. (A) Anesthetized mice were placed on a stand and their eyes were help open in contact with the Micron IV OCT instrument. The focus dials were adjusted to bring the corneal layer into view and images were taken. (B) A graph representing the epithelial, stromal and total thickness of the cornea pre and post 4 weeks of either BX795 or TFT treatment. Two-way ANOVA with Dunnett's multiple comparison test, *** $p < 0.001$ was conducted (n=5 replicates).

559